

Magnetic, thermodynamic, NMR, and transport properties of the heavy-fermion semiconductor U_2Ru_2Sn

V. H. Tran,* S. Paschen,† A. Rabis, N. Senthilkumaran, M. Baenitz, and F. Steglich
Max Planck Institute for Chemical Physics of Solids, D-01187 Dresden, Germany

P. de V. du Plessis
School of Physics, University of the Witwatersrand, P.O. Wits 2050, Johannesburg, South Africa

A. M. Strydom
Physics Department, Rand Afrikaans University, P.O. Box 524, Johannesburg, South Africa
 (Received 19 September 2002; published 28 February 2003)

We have measured the magnetic susceptibility, specific heat, NMR, electrical resistivity, magnetoresistance, Hall effect, thermoelectric power, and thermal conductivity of polycrystalline U_2Ru_2Sn . Some of these properties are compared to those of Th_2Ru_2Sn . The experimental data indicate the formation of a narrow energy gap of approximately $k_B \times 160$ K in U_2Ru_2Sn . Similarities to the behavior of heavy-fermion semiconductors (Kondo insulators) are observed, in particular to CeNiSn. Thus, we believe that U_2Ru_2Sn may be classified as a heavy-fermion semiconductor.

DOI: 10.1103/PhysRevB.67.075111

PACS number(s): 71.27.+a, 72.15.-v, 65.40.-b

I. INTRODUCTION

Heavy-fermion (HF) semiconductors, also referred to as Kondo insulators, show interesting electronic properties due to the opening of a narrow energy gap at the Fermi level at low temperatures.^{1,2} CeNiSn, as one of the most investigated HF semiconductors, is found to have a gap of about 14 K.^{3,4} Other Ce-based compounds, such as $Ce_3Bi_4Pt_3$ (Ref. 5) and CeRhSb (Ref. 6 and 7), are found to possess only slightly larger gaps (~ 40 K). On the other hand, uranium-based HF semiconductors seem to have much larger gaps, even as high as 1000 K.¹ A possible origin of the gap opening in these systems is the hybridization between a half-filled conduction band and an f -electron-derived band.¹ According to this model, a narrow gap is formed only if exactly one half-filled band interacts with one occupied f level. Since at temperatures well below the temperature of the energy gap the numbers of up and down spins in the hybridized band are equal, the magnetic susceptibility must vanish. The electronic coefficient of the specific heat vanishes, too, and the transport properties have the features of a semiconductor. This model explains most of the physical properties of cubic systems such as, for example, $Ce_3Bi_4Pt_3$. This may be due to the fact that the above conditions for gap formation are more likely fulfilled in cubic materials. The only noncubic Kondo insulators known to date are orthorhombic CeNiSn and the isostructural systems CeRhSb and CeRhAs. A slight failure of the conditions for gap formation may be the reason why some low-temperature properties observed in CeNiSn deviate from the above predictions: For example, there exists a metallic T^2 dependence of the electrical resistivity,⁸ a finite value of the electronic specific heat coefficient [$40 \text{ mJ}/(\text{mol K})^2$ at 0.2 K],⁹ and an NMR relaxation rate that returns to a Korringa law below 1 K.⁴

The tetragonal compound U_2Ru_2Sn was considered as a weakly temperature-dependent paramagnet in earlier studies

by Havela *et al.*¹⁰ However, Menon *et al.*¹¹ found that the electrical resistivity shows a maximum at about 170 K, a minimum near 30 K, and an increase towards lower temperatures. Between 13 and 20 K and between 4 and 6 K the resistivity was described by an activation relation, yielding an energy gap of 2 and 0.2 K, respectively, which they took as an indication of Kondo semiconducting behavior. Furthermore, it has been shown¹² that the magnetic susceptibility of U_2Ru_2Sn can be described by the so-called interconfiguration fluctuation model applicable to intermediate valence compounds.¹³

The present paper reports in detail on bulk (magnetic susceptibility and magnetization, specific heat, electrical resistivity, magnetoresistance, Hall coefficient, thermoelectric power, and thermal conductivity) and NMR properties of polycrystalline U_2Ru_2Sn in wide temperature and field ranges. Where appropriate, we compare the results with those for the non- f -electron reference compound Th_2Ru_2Sn . We show that the observed physical properties can be interpreted in terms of the formation of a gap at the Fermi level. Specific heat and ¹¹⁹Sn NMR data allow us to estimate an energy gap of about $k_B \times 160$ K. Thus, U_2Ru_2Sn appears to be the first tetragonal Kondo insulator, and among uranium-based Kondo insulators, it has the smallest energy gap. Part of this work has already been presented at conferences.^{14,15}

II. EXPERIMENTAL DETAILS

Polycrystalline samples of U_2Ru_2Sn and Th_2Ru_2Sn were synthesized as described in Ref. 11, using metals of the following purity in weight %: U, 99.98; Th, 99.99; Ru, 99.97, and Sn, 99.999. In this work we investigated samples obtained from different batches, denoted as sample 1 and sample 2. X-ray diffraction studies showed that, within the usual 5% error, the samples are single phase, crystallizing in the tetragonal U_3Si_2 -type structure (space group $P4/mbm$). Metallographic examination of sample 1, however, revealed

the presence of an impurity phase which we tentatively ascribe to URuSn, amounting to approximately 4% of the total mass of the sample.

The dc magnetic susceptibility was measured by means of a superconducting quantum interference device (SQUID) magnetometer in fields up to 5 T and in the temperature range 2–400 K. Specific-heat measurements were performed in the temperature range 1.8–300 K, utilizing a relaxation-type method. ^{119}Sn NMR measurements were performed on polycrystalline powder samples. The NMR spectra were obtained by Fourier-transforming the digitized spin echoes using a conventional pulsed NMR spectrometer (Bruker, MSL 300, $B=7.05$ T). The spin-lattice relaxation rate was measured by observing the spin-echo recovery after a saturation pulse. The electrical resistivity was measured using a four-probe ac technique in the temperature range 1.8–400 K. The samples were of rectangular shape with typical dimensions $0.5\text{ mm} \times 0.5\text{ mm} \times 5\text{ mm}$. Magnetoresistance and Hall coefficient data were collected in two different ways: Isofield data as a function of temperature in a fixed magnetic field of 13 T on zero-field-cooled samples and isothermal data as a function of field up to 13 T at several selected temperatures below 300 K. Thermopower (2–300 K) and thermal conductivity (2–200 K) were measured with a steady-state method.

III. RESULTS AND DISCUSSION

The general features of the dc magnetic susceptibility $\chi = M/H$ of our two samples of $\text{U}_2\text{Ru}_2\text{Sn}$ measured in a field of 5 T (not shown here) are a Curie-Weiss-type behavior above 200 K and a broad maximum at approximately 170 K, as already shown in Refs. 12 and 14. However, the parameters of the Curie-Weiss law varied considerably between the two samples and for different orientations of the samples with respect to the magnetic field. We suspected that this is due to magnetocrystalline anisotropy together with some texture in the polycrystalline samples. Therefore, we powdered part of sample 2, oriented it in a field of 5 T, and stabilized the oriented powder by embedding it in epoxy. Data of $\chi(T)$ measured with the orientation axis either parallel or perpendicular to the field direction are displayed in Fig. 1. We ascribe the occurrence of a broad maximum followed by a decrease of $\chi(T)$ at lower temperatures to the opening of an energy gap. The weak temperature dependence of $\chi(T)$ of $\text{Th}_2\text{Ru}_2\text{Sn}$ supports this interpretation. In Fig. 2 we show isothermal magnetization curves $M(B)$ of sample 1. The magnetization is very small and varies almost linearly with field.

In zero-field-cooled measurements of $\chi(T)$ with fields smaller than 3 T we observe an anomaly below approximately 60 K. This anomaly may be associated with a ferromagnetic impurity phase, for example, URuSn with $T_C = 60$ K (Ref. 16) or, alternatively, USn with $T_C = 55$ K (Ref. 17). The anomaly is smaller for sample 1 than for sample 2 and the powder, indicating that sample 1 is of higher purity.

Figure 3 shows the temperature dependence of the specific heat, $C_p(T)$, for $\text{U}_2\text{Ru}_2\text{Sn}$ sample 1 and $\text{Th}_2\text{Ru}_2\text{Sn}$. Within the experimental error, the $C_p(T)$ data of sample 2 (not shown) are identical to those of sample 1. By fitting a

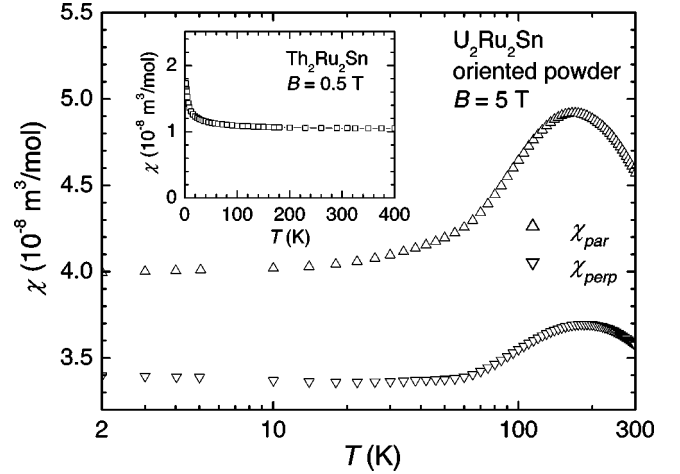


FIG. 1. Temperature dependence of the magnetic susceptibility of an epoxy-stabilized oriented powder sample of $\text{U}_2\text{Ru}_2\text{Sn}$ (part of sample 2). The inset shows the temperature dependence of the magnetic susceptibility of $\text{Th}_2\text{Ru}_2\text{Sn}$.

$C_p(T)/T = \gamma + \beta T^2$ dependence to the data of $\text{U}_2\text{Ru}_2\text{Sn}$ sample 1 at $T < 4$ K one obtains a Sommerfeld coefficient of the electronic specific heat, γ , of $9\text{ mJ}/[(\text{mol U})\text{K}^2]$ for $\text{U}_2\text{Ru}_2\text{Sn}$ and $6\text{ mJ}/[(\text{mol Th})\text{K}^2]$ for $\text{Th}_2\text{Ru}_2\text{Sn}$. The γ value for $\text{U}_2\text{Ru}_2\text{Sn}$ is strikingly small compared to the ones of other U-based 2:2:1 compounds.¹⁰ A natural explanation for this fact is the low density of states, related to the (pseudo)gap at the Fermi level. For the analysis of the lattice specific heat of $\text{Th}_2\text{Ru}_2\text{Sn}$ we have fitted a Debye function to the experimental data above 50 K. This fit yields a Debye temperature of approximately 210 K, the same value as estimated from the β value of $0.5\text{ mJ}/[(\text{mol U})\text{K}^4]$. At temperatures where the electronic contributions are small (above 6 K) the magnetic contribution to the specific heat of $\text{U}_2\text{Ru}_2\text{Sn}$ was obtained as $C_{mag} = C_{\text{U}_2\text{Ru}_2\text{Sn}} - C_{\text{Th}_2\text{Ru}_2\text{Sn}}$. It may reasonably well be approximated with the relation

$$C_{Sch} = R \left(\frac{\Delta}{2k_B T} \right)^2 \frac{\exp(-\Delta/2k_B T)}{1 + \exp(-\Delta/2k_B T)^2}. \quad (1)$$

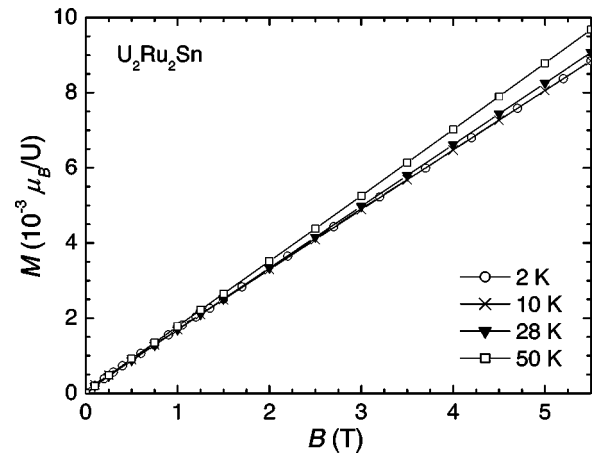


FIG. 2. Isothermal magnetization of $\text{U}_2\text{Ru}_2\text{Sn}$ (sample 1) as a function of magnetic field.

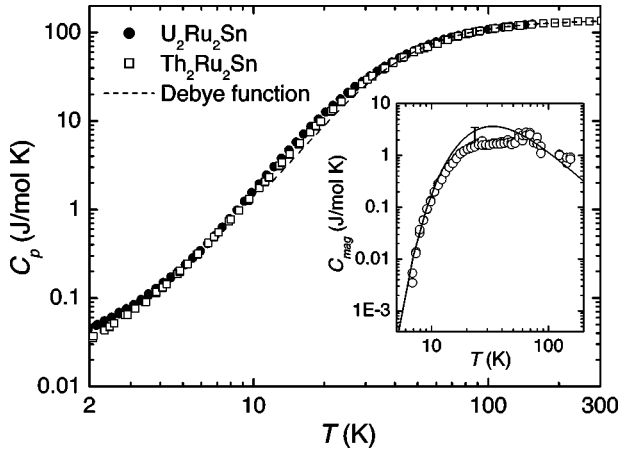


FIG. 3. Temperature dependence of the specific heat of U_2Ru_2Sn (sample 1) and Th_2Ru_2Sn . The dashed line represents the Debye function. The inset shows the magnetic contribution of the specific heat $C_{mag} = C_{U_2Ru_2Sn} - C_{Th_2Ru_2Sn}$. The solid line presents the specific heat associated with the Schottky anomaly (see text).

Such a Schottky-type relation accounts for a band model with two very narrow density of states (DOS) peaks on either side of the gap,² frequently evoked for Kondo insulators. The energy gap Δ extracted from our fit is $k_B \times 160$ K. The deviations from the fit are attributed to the large error resulting from subtracting from one another two quantities of similar magnitudes.

Strong support for the formation of a gap is given by the temperature dependence of the spin-lattice relaxation rate, $1/T_1(T)$, obtained in ^{119}Sn NMR measurements at 7 T. As can be seen from Fig. 4, below approximately 200 K, $1/T_1$ for U_2Ru_2Sn decreases by two orders of magnitude. As a first approach we describe $1/T_1$ vs T between 40 and 220 K by an exponential curve $1/T_1 \propto \exp(-\Delta/k_B T)$, yielding the energy gap $\Delta = k_B \times 155$ K. This relation is known to describe the energy gap of spin-Peierls systems or conventional

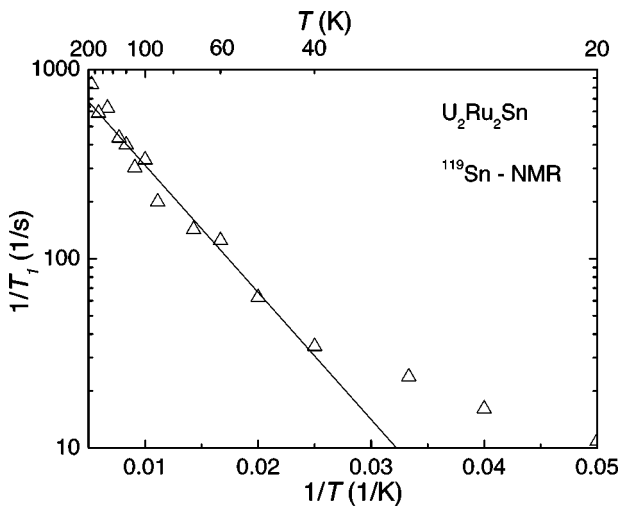


FIG. 4. ^{119}Sn NMR spin-lattice relaxation rate of U_2Ru_2Sn powder (from sample 2) plotted as a function of inverse temperature. The straight line indicates a simple exponential behavior which corresponds to a gap value of 155 K.

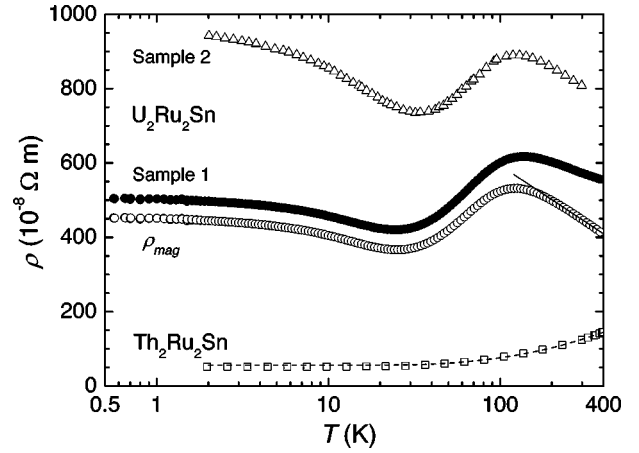


FIG. 5. Temperature dependence of the electrical resistivity of U_2Ru_2Sn and Th_2Ru_2Sn . The data of Th_2Ru_2Sn are fitted using a Bloch-Grüneisen-Mott equation. Also depicted is the magnetic resistivity of U_2Ru_2Sn (sample 1) calculated from $\rho_{mag} = \rho_{U_2Ru_2Sn} - \rho_{Th_2Ru_2Sn}$.

superconductors. A fit of this relation to the published data of $CeNiSn$ (Ref. 4) gives $\Delta = k_B \times 14$ K, i.e., an approximately one order of magnitude smaller value than for U_2Ru_2Sn . Below 10 K, $1/T_1$ of U_2Ru_2Sn is linear in T . The low-temperature deviation from an exponential curve and the $1/T_1 \propto T$ law observed in $CeNiSn$ below $T \approx 0.3$ K has been ascribed to a “V-shaped” gap in combination with a residual density of states within the gap.⁴ The same interpretation may hold for U_2Ru_2Sn .

In Fig. 5 we compare the temperature dependence of the electrical resistivity, $\rho(T)$, of U_2Ru_2Sn with that of Th_2Ru_2Sn . The resistivity of Th_2Ru_2Sn decreases smoothly with decreasing temperature. It is clear that scattering in this case is to be attributed mainly to phonons. Therefore, we may analyze the experimental data by using a Bloch-Grüneisen-Mott expression¹⁸

$$\rho(T) = \rho_0 + 4aT \left(\frac{T}{\Theta_D} \right)^4 \times \int_0^{\Theta_D/T} \frac{x^5}{[\exp(x) - 1][\exp(-x) - 1]} dx - bT^3, \quad (2)$$

where Θ_D is the Debye temperature and a and b are constants. The last term in this equation describes interband scattering processes. In fitting Eq. (2) to our experimental data we used the Debye temperature obtained from our specific-heat measurements. The dashed line in Fig. 5 illustrates such a fit with $a = 0.257 \mu\Omega \text{ cm/K}$ and $b = 1.97 \times 10^{-7} \mu\Omega \text{ cm/K}^3$. The excellent fit implies that Th_2Ru_2Sn is a good phonon reference for U_2Ru_2Sn . The temperature dependence of ρ is similar for both U_2Ru_2Sn samples and is in overall agreement with that in Refs. 11 and 12. The fact that the absolute values of sample 1 and 2 differ by almost a factor of 2 may be attributed to different porosities of the two samples, giving rise to different effective geometric factors.

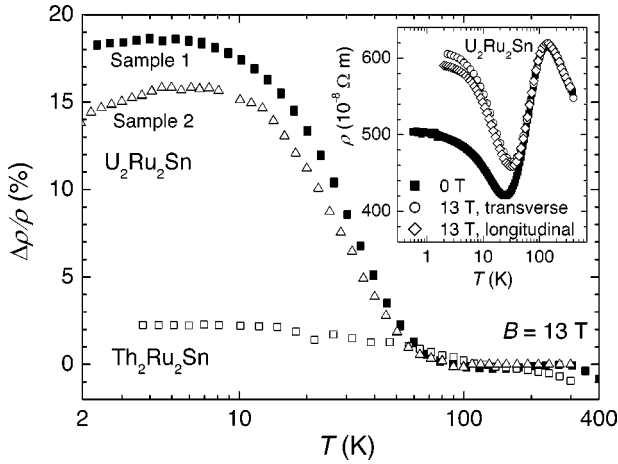


FIG. 6. Temperature dependence of the transverse magnetoresistance of U_2Ru_2Sn and Th_2Ru_2Sn obtained in a field of 13 T. The inset shows the resistivity data for U_2Ru_2Sn (sample 1) at 0 and 13 T for both the transverse and the longitudinal configuration.

Thus, the absolute values of ρ shown in Fig. 5 should be taken as upper boundaries for ρ of bulk U_2Ru_2Sn . The magnetic resistivity of U_2Ru_2Sn , $\rho_{mag} = \rho_{U_2Ru_2Sn} - \rho_{Th_2Ru_2Sn}$, obtained for sample 1 displays a logarithmic dependence between 200 and 400 K, has a maximum at approximately 125 K, and drops strongly below that temperature. Similar behavior was observed for CeNiSn and CeRhSb (Ref. 19), where the drop was attributed to the onset of coherence. Below $T_{min} = 25$ K, $\rho(T)$ shows an upturn and tends to saturate with further decreasing temperature below 1 K. The saturation of ρ_{mag} at low temperatures may be related to the non-cubic crystal structure of U_2Ru_2Sn , as discussed for CeNiSn in the Introduction. It is, at first sight, surprising that, below the temperature where the energy gap is believed to open, we observe a decrease of $\rho(T)$ rather than an increase. As we shall show below, the Hall effect data resolve this puzzle: The reduction of the charge-carrier concentration is overcompensated by a gain in mobility.

The influence of magnetic fields on the resistivity is displayed in Fig. 6 for Th_2Ru_2Sn and U_2Ru_2Sn . In transverse magnetic fields of 13 T, ρ of Th_2Ru_2Sn is altered only slightly. The transverse magnetoresistance of this compound reaches a value of about 2.5% at 3 K, typical of a normal metal. In contrast, for U_2Ru_2Sn one observes a big difference between $\rho(T, B=0)$ and $\rho(T, B=13$ T) just below 50 K, both for the transverse and for the longitudinal configuration (see inset of Fig. 6). The small difference between $\rho(T, B=13$ T, transverse) and $\rho(T, B=13$ T, longitudinal) may be attributed to an extra positive contribution for the transverse configuration due to the cyclotron motion of conduction electrons. In addition to the enhancement of ρ , leading to a positive magnetoresistance of about 18% at 2 K and 13 T for the transverse configuration (Fig. 6), the field shifts also T_{min} towards higher temperature. The transverse magnetoresistance results of sample 2 are qualitatively similar to those for sample 1, but the $\Delta\rho(B)/\rho$ value is somewhat smaller. We obtained 14% at 2 K and 13 T for this sample. We thus conclude that the magnitude of the transverse magnetoresis-

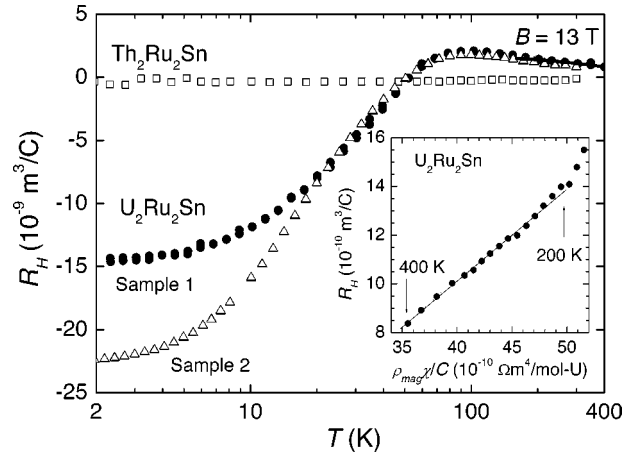


FIG. 7. Temperature dependence of the Hall coefficient of U_2Ru_2Sn and Th_2Ru_2Sn obtained in a field of 13 T. Inset: the high-temperature part of the Hall coefficient of U_2Ru_2Sn (sample 1) as a function of $\rho_{mag}\chi/C$. The solid line in both the main figure and the inset is a fit (see text).

tance is sample dependent, while the general temperature and field (not shown) dependence is the same for the two different samples. One might argue that a small amount of a ferromagnetic impurity phase is responsible for the large magnetoresistance. However, ferromagnetic URuSn has a negative magnetoresistance.²⁰ Thus, the origin of the large positive transverse and longitudinal magnetoresistance in our U_2Ru_2Sn samples is not understood at present. A large positive transverse magnetoresistance has also been reported for a high-quality sample of CeNiSn for $H||b$ and c axis in fields up to 15 T,²¹ where it was explained by the cyclotron motion of the compensated carriers. A negative magnetoresistance has been observed for CeNiSn in the $H||a$ axis configuration and was ascribed to a gradual field-induced decrease of the anisotropic hybridization gap.²¹

In Fig. 7 we show the temperature dependence of the Hall coefficient, $R_H(T)$, for Th_2Ru_2Sn and U_2Ru_2Sn . While R_H of Th_2Ru_2Sn is practically temperature independent, R_H of U_2Ru_2Sn displays a strong temperature dependence below $T_{max} = 102$ K. For both U_2Ru_2Sn and Th_2Ru_2Sn the room-temperature Hall resistivity $\rho_H = R_H B$ varies linearly with the magnetic field. The negative slope of $1.1 \times 10^{-10} \text{ m}^3/\text{C}$ for Th_2Ru_2Sn indicates n -type conduction. For U_2Ru_2Sn , it is not obvious to ascribe the positive slope of $1.1 \times 10^{-9} \text{ m}^3/\text{C}$ to p -type conduction because, for magnetic systems, the Hall coefficient is generally a combination of two contributions: The normal Hall coefficient R_0 resulting from the Lorentz motion of carriers and the extraordinary one originating from magnetic scattering of these carriers: $R_H = R_0 + R_e$. According to Fert and Levy²² the Hall coefficient for heavy-fermion compounds in the incoherent state, calculated under the assumption of dominating skew scattering, is given by

$$R_H = R_0 + \gamma_1 \tilde{\chi} \rho_m, \quad (3)$$

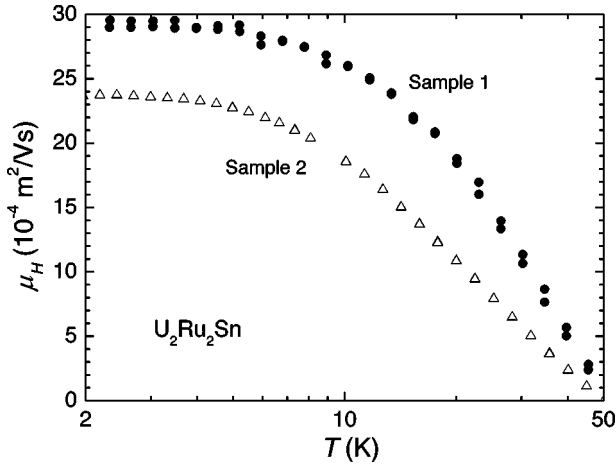


FIG. 8. Temperature dependence of the Hall mobility calculated as the ratio R_H/ρ .

where ρ_m is the magnetic resistivity, $\tilde{\chi} = \chi/C$, and C is the Curie constant. The coefficient γ_1 , related to the phase shift δ_2 , takes the form

$$\gamma_1 = -\frac{5}{7} g \mu_B k_B^{-1} \sin \delta_2 \cos \delta_2. \quad (4)$$

Though for Kondo insulators a temperature-independent R_0 is not, *a priori*, anticipated we shall assume that R_0 is essentially constant between 200 and 400 K for this analysis. In this temperature range, the experimental data of the Hall coefficient can be described by Eqs. (3) and (4) with $R_0 = -5 \times 10^{-10} \text{ m}^3/\text{C}$ and $\gamma_1 = 0.38 \text{ K/T}$. The result of the fit is shown in Fig. 7 as a solid line, as well as in the inset. The good quality of the fit suggests that, indeed, the temperature dependence of R_H is mainly due to incoherent skew scattering by the U $5f$ moments at high temperatures. The carrier concentration estimated from R_0 in a one-band model is $n_e = 1.2 \times 10^{28} \text{ m}^{-3}$, corresponding to 1.2 electrons per $\text{U}_2\text{Ru}_2\text{Sn}$ formula unit. As coherence sets in, the incoherent skew scattering in $\text{U}_2\text{Ru}_2\text{Sn}$ will no longer be dominant, and a sign reversal of the Hall coefficient is expected and indeed observed near 50 K. Interestingly, a sign change in $R_H(T)$ has also been observed for CeNiSn (Ref. 8). In the case of $\text{U}_2\text{Ru}_2\text{Sn}$, below 50 K, ρ_H is no longer linear in field. The origin of this behavior is not clear at present. At 2 K and 13 T, $R_H(T)$ of sample 1 reaches a value of $-1.45 \times 10^{-8} \text{ m}^3/\text{C}$. In a one-band model, this corresponds to an electron concentration of $4.3 \times 10^{26} \text{ m}^{-3}$ or to 0.04 electrons per $\text{U}_2\text{Ru}_2\text{Sn}$ formula unit. The fact that $R_H(2 \text{ K})$ of sample 2 differs considerably from that of sample 1 may be attributed to differences in the sample quality (e.g., different residual charge-carrier concentrations). In Fig. 8 we show the temperature dependence of the Hall mobility, $\mu_H = R_H/\rho$. Keeping in mind that we believe R_H to be dominated by the extraordinary contribution at high temperatures, μ_H obtained in this way is relevant only below the temperature where $R_H(T) = R_0$, i.e., below 50 K. μ_H of both $\text{U}_2\text{Ru}_2\text{Sn}$ samples increases strongly with decreasing temperature reaching 30

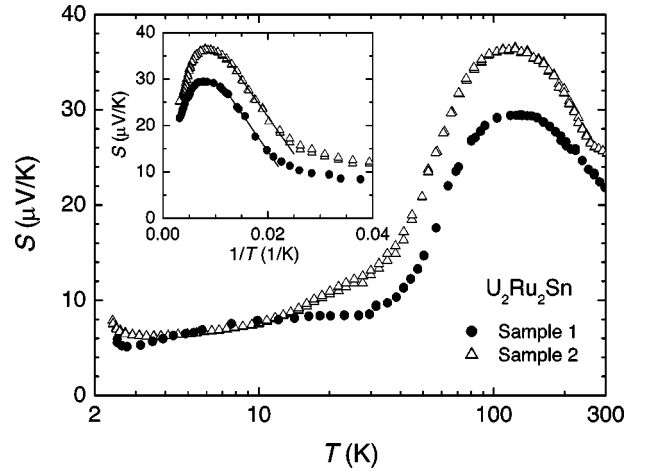


FIG. 9. Temperature dependence of the thermoelectric power of $\text{U}_2\text{Ru}_2\text{Sn}$. The inset shows S vs $1/T$. The lines represent fits of Eq. (5) to these data.

$\text{cm}^2/(\text{V s})$ for sample I at 2 K. As for CeNiSn and CeRhSb (Ref. 8), μ_H of $\text{U}_2\text{Ru}_2\text{Sn}$ follows approximately a $\ln T$ law between 15 and 50 K.

The temperature dependence of the thermoelectric power, $S(T)$, is shown in Fig. 9. In both samples of $\text{U}_2\text{Ru}_2\text{Sn}$, $S(T)$ is positive in the investigated temperature range. The most remarkable features are a maximum at approximately 120 K with a relatively large value of 30 to 35 $\mu\text{V/K}$ and a smaller anomaly at 10–20 K. Such a two-peak structure of $S(T)$ has already been observed for CeNiSn (Ref. 3) and CeRhSb (Ref. 23). The large value of $S(T)$ cannot be explained by a diffusion contribution only. Taking the above-determined Hall coefficient R_0 we estimate the diffusion thermopower to be 11 $\mu\text{V/K}$, which is 2 times smaller than the experimental value. Instead, we associate the occurrence of the high-temperature maximum with the formation of the energy gap, as was done for $\text{Ce}_3\text{Bi}_4\text{Pt}_3$ in Ref. 24. For a semiconductor, the thermoelectric power is given by²⁵

$$S(T) = \frac{k_B}{e} \left(\frac{\Delta}{2k_B T} + \frac{5}{2} + r \right), \quad (5)$$

where r is a constant and e the electronic charge including sign. The inset of Fig. 9 illustrates that an inverse temperature behavior is valid for the $S(T)$ curves in a temperature range 45–75 K. The fit of Eq. (5) to these curves yields a gap of about 40 K, which is distinctly smaller than the value estimated from the $C_p(T)$ and NMR data. This may be related to the presence of a residual density of states within the gap. The origin of the low-temperature $S(T)$ anomaly is not clear at present. Usually, one considers similar anomalies to be due to a phonon-drag mechanism, where such a kind of maximum occurs in the temperature range $(0.1-0.2) \times \Theta_D$. For $\text{U}_2\text{Ru}_2\text{Sn}$, $\Theta_D \sim 210 \text{ K}$ and the anomaly would be expected in the temperature range between 20 and 40 K, slightly higher than observed experimentally.

The temperature dependence of the thermal conductivity, $\kappa(T)$, of two samples of $\text{U}_2\text{Ru}_2\text{Sn}$ is shown in Fig. 10. We

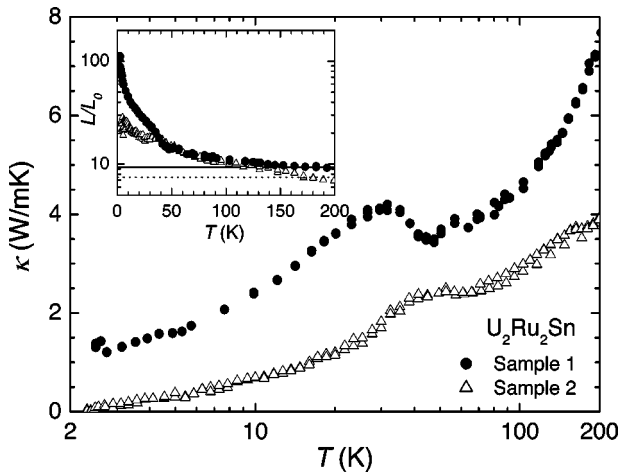


FIG. 10. Temperature dependence of the thermal conductivity of U_2Ru_2Sn . The inset shows the reduced Lorenz number as a function of temperature. The solid and dotted lines are constant fits to the data above 160 K.

see that the absolute value of $\kappa(T)$ is distinctly different for the two samples. As in the case of $\rho(T)$ (cf. Fig. 5), we suspect that the smaller $\kappa(T)$ values of sample 2 are due to an uncertainty in the geometric factor. It can be seen that $\kappa(T)$ decreases smoothly between 200 and 50 K, where it suddenly increases and then passes over a maximum at approximately 30 K. The latter feature is more pronounced in sample 1. In the inset of Fig. 10 we show the reduced Lorenz number $L(T)/L_0$, where $L(T) = \rho(T)\kappa(T)/T$ and $L_0 = 2.45 \times 10^{-8} \text{ (V/K)}^2$. In the entire temperature range, $L(T)/L_0$

has a large value, indicating that $\kappa(T)$ is dominated by phonons. A more pronounced increase of $L(T)/L_0$ sets in below approximately 160 K. This enhancement of $L(T)/L_0$ is similar to that found for $CeNiSn$ and $CeRhSb$ where it was ascribed to an increase of the relaxation time of the phonons as a result of the decrease of the concentration of charge carriers, which are the dominant phonon scatterers.^{26,27} In other words, the enhancement of $L(T)/L_0$ is related to the opening of the gap at the Fermi level.

IV. CONCLUSION

We have reported bulk and microscopic measurements for polycrystalline samples of the tetragonal compound U_2Ru_2Sn . The magnetic susceptibility, specific heat, NMR, electrical resistivity, Hall coefficient, thermoelectric power, and thermal conductivity results show many similarities to the behavior observed in other HF semiconductors. The energy gap in U_2Ru_2Sn estimated from the specific heat and NMR measurements is approximately of $k_B \times 160$ K. A first hint for a non-negligible anisotropy of U_2Ru_2Sn comes from magnetic susceptibility measurements on oriented powder. Whether the anisotropic susceptibility is due to an anisotropy of the energy gap remains to be revealed by future experiments on U_2Ru_2Sn single crystals.

ACKNOWLEDGMENT

The authors thank Professor J. Mydosh for providing the results of the microanalysis study of the samples.

*Present address: Trzebiatowski Institute of Low Temperature and Structure Research, Polish Academy of Sciences, 50–950 Wrocław, Poland.

†Corresponding author.

¹G. Aeppli and Z. Fisk, *Comments Condens. Matter Phys.* **16**, 155 (1992).

²P. S. Riseborough, *Adv. Phys.* **49**, 257 (2000).

³T. Takabatake, F. Teshima, H. Fujii, S. Nishigori, T. Suzuki, T. Fujita, Y. Yamaguchi, J. Sakurai, and D. Jaccard, *Phys. Rev. B* **41**, 9607 (1990).

⁴K. Nakamura, Y. Kitaoka, K. Asayama, T. Takabatake, G. Nakamoto, H. Tanaka, and H. Fujii, *Phys. Rev. B* **53**, 6385 (1996).

⁵M. F. Hundley, P. C. Canfield, J. D. Thompson, Z. Fisk, and J. M. Lawrence, *Phys. Rev. B* **42**, 6842 (1990).

⁶S. K. Malik and D. T. Adroja, *Phys. Rev. B* **43**, 6277 (1991).

⁷S. K. Malik, L. Menon, V. K. Pecharsky, and K. A. Gschneidner, *Phys. Rev. B* **55**, 11 471 (1997).

⁸T. Takabatake, G. Nakamoto, T. Yoshino, H. Fujii, K. Izawa, S. Nishigori, H. Goshima, T. Suzuki, T. Fujita, K. Maezawa, T. Hiraoka, Y. Okayama, I. Oguro, A. A. Menovsky, K. Neumaier, A. Brückl, and K. Andres, *Physica B* **223-22**, 413 (1996); T. Takabatake, F. Iga, T. Yoshino, Y. Echizen, K. Katoh, K. Kobayashi, M. Higa, N. Shimizu, Y. Bando, G. Nakamoto, H. Fujii, K. Izawa, T. Suzuki, T. Fujita, M. Sera, M. Hiroi, K. Maezawa, S. Mock, H. v. Löhneysen, A. Brückl, K. Neumaier, and K. Andres, *J. Magn. Magn. Mater.* **177-181**, 277 (1998).

⁹K. Izawa, T. Suzuki, T. Fujita, T. Takabatake, G. Nakamoto, H. Fujii, and K. Maezawa, *Phys. Rev. B* **59**, 2599 (1999).

¹⁰L. Havela, V. Sechovský, P. Svoboda, H. Nakotte, K. Prokeš, F. R. de Boer, A. Seret, J. M. Winand, J. Rebizant, J. C. Spirlet, A. Purwanto, and R. A. Robinson, *J. Magn. Magn. Mater.* **140-144**, 1367 (1995).

¹¹L. Menon, P. de V. du Plessis, and A. M. Strydom, *Solid State Commun.* **106**, 519 (1998).

¹²P. de V. du Plessis, A. M. Strydom, R. Troć, and L. Menon, *J. Phys.: Condens. Matter* **13**, 8375 (2001).

¹³B. C. Sales and D. K. Wohlleben, *Phys. Rev. Lett.* **35**, 1240 (1975).

¹⁴V. H. Tran, S. Paschen, A. Rabis, M. Baenitz, F. Steglich, P. de V. du Plessis, and A. M. Strydom, *Physica B* **312-313**, 215 (2002).

¹⁵S. Paschen, M. Baenitz, V. H. Tran, A. Rabis, F. Steglich, W. Carrillo-Cabrera, Yu. Grin, A. M. Strydom, and P. de V. du Plessis, *J. Phys. Chem. Solids* **63**, 1183 (2002).

¹⁶V. H. Tran and R. Troć, *J. Magn. Magn. Mater.* **102**, 74 (1991).

¹⁷P. Boulet and H. Noël, *Solid State Commun.* **107**, 135 (1998).

¹⁸N. F. Mott and H. Jones, *The Theory of the Properties of Metals and Alloys* (Oxford University Press, London, 1958), p. 240.

¹⁹D. T. Adroja, B. D. Rainford, A. J. Neville, P. Mandal, and A. G. M. Jansen, *J. Magn. Magn. Mater.* **161**, 157 (1996).

²⁰V. H. Tran, R. Troć, and D. Badurski, *J. Alloys Compd.* **219**, 285 (1995).

²¹Y. Inada, T. Ishida, H. Azuma, D. Aoki, R. Settai, Y. Onuki, K.

- Kobayashi, T. Takabatake, G. Nakamoto, H. Fujii, and K. Maezawa, *Physica B* **230-232**, 690 (1997).
- ²²A. Fert and P. M. Levy, *Phys. Rev. B* **36**, 1907 (1987).
- ²³T. Takabatake, H. Tanaka, Y. Bando, H. Fujii, S. Nishigori, T. Suzuki, T. Fujita, and G. Kido, *Phys. Rev. B* **50**, 623 (1994).
- ²⁴M. F. Hundley, P. C. Canfield, J. D. Thompson, and Z. Fisk, *Phys. Rev. B* **50**, 18 142 (1994).
- ²⁵N. F. Mott, *Conduction in Non-Crystalline Materials* (Clarendon, Oxford, 1987); N. F. Mott, *Metal-Insulator Transitions* (Taylor & Francis, London, 1990).
- ²⁶M. Sera, N. Kobayashi, T. Yoshino, K. Kobayashi, T. Takabatake, G. Nakamoto, and H. Fujii, *Phys. Rev. B* **55**, 6421 (1997).
- ²⁷S. Paschen, B. Wand, G. Sparr, F. Steglich, Y. Echizen, and T. Takabatake, *Phys. Rev. B* **62**, 14 912 (2000).